

Rapid fabrication of diffusion barrier between metal electrode and thermoelectric materials using current-controlled spark plasma sintering technique

FERRERES, Xavier and AMINORROAYA YAMINI, Sima
<<http://orcid.org/0000-0002-2312-8272>>

Available from Sheffield Hallam University Research Archive (SHURA) at:
<http://shura.shu.ac.uk/19052/>

This document is the author deposited version. You are advised to consult the publisher's version if you wish to cite from it.

Published version

FERRERES, Xavier and AMINORROAYA YAMINI, Sima (2018). Rapid fabrication of diffusion barrier between metal electrode and thermoelectric materials using current-controlled spark plasma sintering technique. Journal of Materials Research and Technology.

Copyright and re-use policy

See <http://shura.shu.ac.uk/information.html>

Available online at www.sciencedirect.com

jmr&t
Journal of Materials Research and Technology
www.jmrt.com.br



Original Article

Rapid fabrication of diffusion barrier between metal electrode and thermoelectric materials using current-controlled spark plasma sintering technique

Xavier Reales Ferreres^a, Sima Aminorroaya Yamini^{a,b,*}

^a Australian Institute for Innovative Materials (AIIM), Innovation Campus, University of Wollongong, Squire Way, North Wollongong, NSW 2500, Australia

^b Department of Engineering and Mathematics, Sheffield Hallam University, Sheffield S1 1WB, UK

ARTICLE INFO

Article history:

Received 11 July 2017

Accepted 8 January 2018

Available online xxx

Keywords:

Current-controlled spark plasma sintering

Thermoelectric

Module

Diffusion barrier

Rapid sintering

ABSTRACT

A continuous, stable diffusion barrier between PbTe thermoelectric material and Ni conducting electrode was generated using the current-controlled spark plasma sintering technique. This new method creates a diffusion barrier layer by utilising the melt generated in the area of contact between components, also called the weld nugget in a resistance spot welding process. The current-controlled spark plasma sintering process bonds the solid workpieces in a fraction of the time required to fabricate interphase layers using powder components with the common temperature-controlled spark plasma sintering. The substantially reduced time of bonding compared to previous methods is beneficial to the thermoelectric properties of materials due to their limited exposure to high temperatures, which occasionally are much higher than the operating temperatures of devices. This work introduces a rapid and efficient bonding technique that can be applied to a wide variety of materials.

© 2018 Brazilian Metallurgical, Materials and Mining Association. Published by Elsevier Editora Ltda. This is an open access article under the CC BY-NC-ND license (<http://creativecommons.org/licenses/by-nc-nd/4.0/>).

1. Introduction

The growing influence of climate change [1,2] has triggered environmentally friendly energy generation plants while also increasing their efficiency [3–6]. Thus, thermoelectric generators (TEG) have attracted industry and research interest due

to their capability to harvest waste heat [7–9]. Both n-type and p-type lead telluride (PbTe) are the leading thermoelectric materials within the 700–900 K temperature range for TEG [10,11]. Joining the thermoelectric materials to a metallic electrode is crucial, however, for the performance of high temperature devices [12], since the maximum operating temperatures and generated power of a TEG are dependent on the preservation of ohmic contact [13].

Conventional joining techniques such as soldering and brazing are still used in low to mid temperature range

* Corresponding author.

E-mail: S.Aminorroaya@shu.ac.uk (S. Aminorroaya Yamini).

<https://doi.org/10.1016/j.jmrt.2018.01.008>

2238-7854/© 2018 Brazilian Metallurgical, Materials and Mining Association. Published by Elsevier Editora Ltda. This is an open access article under the CC BY-NC-ND license (<http://creativecommons.org/licenses/by-nc-nd/4.0/>).

applications in order to connect the conducting electrode to the thermoelectric material [14]. Due to the strong reactions and diffusion of elements at the contact at high operating temperatures, however, new bonding methods need to be adopted to meet critical contact requirements, including low resistivity, high temperature stability, and reproducibility of the diffusion barrier structure [15]. Powder consolidating equipment, such as in hot pressing (HP) and electric-current-assisted sintering methods such as spark plasma sintering (SPS), has been used to form reliable contacts [16,17]. It is the latter technology; however, that is drawing more attention due to its two notable advantages of low sintering temperatures and short consolidation time compared to HP. These advantages achieved in SPS are caused by the intrinsic electrical current in the apparatus, which via Joule heating and under a uniaxial force on the sample produces high density bulk products with improved mechanical properties [18]. Nickel electrode has been bonded directly to PbTe and formed a diffusion barrier layer composed of β_2 $\text{Ni}_{3\pm x}\text{Te}_2$ phase, using the commonly practiced temperature-controlled SPS method [19]. We have previously bonded PbTe to Ni using a “one-step” method that simultaneously sintered the PbTe powder and generated a thick 27 μm interlayer at the contact with the Ni electrode [19]. This layer solely consists of Ni_3Te_2 , which proved to effectively withstand a high temperature ageing process. In order to achieve low contact resistance and therefore improve the total performance of the TEG [15], we then joined Ni to PbTe via a bulk solid-state reaction that resulted in a 7 μm interlayer of Ni_3Te_2 [20]. Observations of large oscillations in the current and voltage, however, appeared to show a negative effect on the final product, generating cracks and porosity in the thermoelectric material. In the current study, we present a new diffusion bonding approach, where the applied electrical current is controlled during spark plasma sintering, instead of the commonly practiced temperature-controlled method. This new approach eliminates oscillations in the current during the process of joining the thermoelectric material to the metal electrode and greatly reduces the required sintering time for the fabrication of the sample. This aids the quality of thermoelectric material through a reduction in cracking and porosity due to the short exposure to Joule heating. Moreover, the successful formation of an effective thin diffusion barrier approximately 3 μm in thickness that is composed solely of Ni_3Te_2 is anticipated to minimise the contribution of electrical contact resistance to the total efficiency of the final thermoelectric generator.

2. Materials and methods

Polycrystalline samples of $\text{PbTe}_{0.9988}\text{I}_{0.0012}$ were synthesised by mixing stoichiometric quantities of high purity Pb (99.999%), Te (99.999%), and PbI_2 in vacuum-sealed quartz ampoules. Samples were heated at 1373 K and homogenised for 10 h, followed by cold water quenching. Subsequently, samples were annealed at 823 K for 72 h. The obtained ingots of n-type lead telluride were hand ground to powder in a protective atmosphere. Powders were then sintered into disks 12 mm in diameter and 1.5 mm in thickness via SPS equipment at 793 K and 40 MPa axial pressure for 1 h under vacuum.

The process for joining the PbTe disks to the Ni plate was conducted via bonding of solid pieces under uniaxial pressures of 10, 20, and 30 MPa in vacuum with different holding times. The faying surfaces were mechanically polished down to a 1 μm surface roughness prior to the bonding procedure. The equipment utilised for the joining of the materials was a Thermal Technology LLC SPS 10-4 with a modified assembly, as detailed in our previous work [20] and illustrated in Figure 1 of the Supporting Information. This new assembly entails the elimination of the graphite die, hence forcing the electrical current to pass through the PbTe and Ni workpieces, and the contact area between them.

The commonly practiced SPS method uses the thermocouple temperature reading to adjust the electrical current required to sinter the initial powders. In comparison, the current study involves direct control of the electrical current by bypassing the original proportional-integral-derivative (PID) controller for temperature-controlled processes and using DC current of 250 A for the bonding. It is worth noting that the equipment's PID controller has a theoretical 6% error at the low currents used in the present study, since this specific equipment is designed to apply currents as high as 4000 A.

The electrical resistance of the interface was measured using the Quantum Design PPMS equipment. The V-I curve was obtained from bonded Ni to PbTe sample to determine the type of contact resistance. Electrical currents used for the measurement were set between 7 mA and 100 mA. The frequencies of 100 Hz were used to avoid any Peltier effect in the sample. The final resistance of interphase and contacts with Ni and PbTe is obtained through subtracting the resistance values of PbTe and Ni plate from the total measured resistance of the Ni + PbTe sample.

The obtained microstructures at the interlayer of bonded samples after different welding times of 10, 15 and 20 s were analysed using a scanning electron microscope (SEM – JEOL JSM 7001F), which was equipped with energy dispersive X-ray spectroscopy (EDS). In order to prepare the cross-sections for analysis, they were mechanically polished down to 1 μm and ion milled for 2 h using a Leica RES 101 Ion Miller.

3. Results and discussion

This study introduces rapid bonding of PbTe and Ni plate using a current-controlled spark plasma sintering technique. This method resembles welding and, in particular, resistance spot welding (RSW) [21], resulting in the generation of molten material between the faying surfaces of the Ni and PbTe. The aim of this study was to utilise the commonly mentioned weld nugget of resistance spot welding as the means to form a diffusion barrier layer at the Ni/PbTe interface for use in thermoelectric application. In order to generate such a layer, the experimental welding parameters, including the electrical current, electrode force, and weld time must be optimised. These parameters are cardinal variables, for both RSW and current-controlled SPS, in order to attain desirable bonding. Nevertheless, other factors such as the electrode material and its geometry also affect the final welding product in RSW processes, whereas in the current-controlled SPS joining process, these elements remain constant. The electrode contact area is

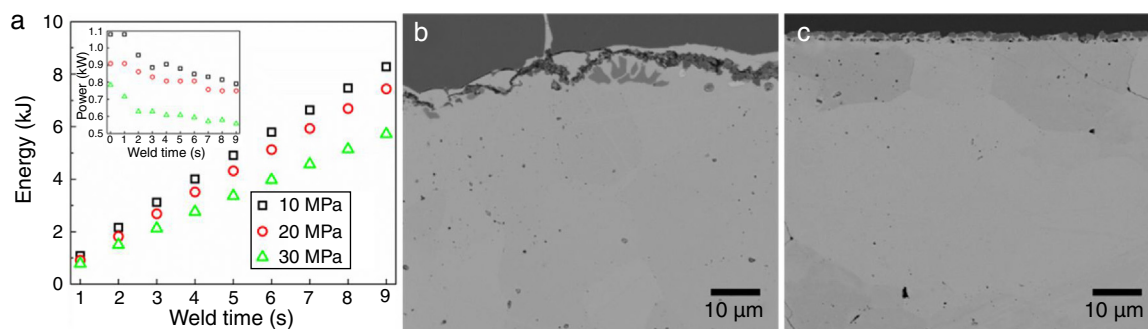


Fig. 1 – (a) Energy supplied by SPS during welding time at pressures of 10, 20 and 30 MPa. Inset in (a) shows the power supplied at different pressures during the welding time. Cross-sections of samples subjected to (b) 10 MPa and (c) 20 MPa. The sample made at 30 MPa showed no occurrence of bonding. This was due to the lower contact resistance induced by the increased pressure.

fixed to an area 12 mm in diameter in this study and the choice of material is graphite, which has lower electrical conductivity compared to the materials used for RSW such as copper [22].

The formation of an optimal interphase, during a similar procedure to RSW, requires an understanding of its primary variables: electrical current, weld time, and electrode force. The welding current is a critical variable for joining methods and often determines the quality of the cross-section and formation of the nugget [23]. A very low current is unable to produce sufficient heat at the contact between the surfaces, while a very high current results in extensive expulsion of molten material and consequently increases the porosity if the boiling point of the material is reached.

Usually in RSW processes, the initial welding parameters are determined based on welders' experience or empirical tables [24], with the variables subsequently tuned according to the quality of the generated nugget, as determined from cross-sections of workpieces. There are no parameters available in the literature, however, for welding Ni to PbTe. Therefore, we have adopted the initial parameters from our recent studies on joining Ni to PbTe using temperature-controlled SPS [19].

The required electrical current value in RSW procedures is often optimised by gradual increases in value until the initial generated melt spatters between the workpieces. An electrical current of approximately 280 A pulsed DC was found to form an interlayer roughly 7.5 μm in thickness in our most recent study [20], which is shown in Figure S3 of the Supporting Information. In comparison, an electrical current of 250 A was obtained as the optimum value in this current study due to the use of direct current instead of pulsed DC. Lower electrical current is advantageous in this particular case, since less Joule heating will be generated on the PbTe side, which is beneficial to its thermoelectric properties [25].

Fig. 1(a) shows the supplied SPS energy during 10 s of bonding at pressures of 10, 20, and 30 MPa. The supplied energy, E (kJ) increases linearly with time in accordance with $E = P \times t$, where P is the instant power (kW), and t the welding time (s). The slope values of the lines in Fig. 1(a) determine the instant power supplied by the SPS equipment. Fig. 1(a) inset presents the variation in the supplied power as a function of welding time, at 10, 20, and 30 MPa. The observed differences in power at $t = 0$ are representative of the variation in the effect of the

applied force on the contact resistance between the Ni and PbTe. It is clear that, at a given electrical current, increasing the pressure and consequently the force requires less supplied electrical power. This is due to the direct relationship between the force and the contact area, which consequently decreases the contact resistance [22]. The force applied on the workpieces by the electrodes must assure sufficient contact during the entire bonding process. A very high force reduces contact resistance, thus decreasing the generated heat, whereas a very low force can cause geometrical instability and expulsion of liquid phase due to disproportionate amounts of heat [26,27]. The requirements for applied forces vary according to the mechanical properties of materials and the quality of the contact area [21]. At higher pressures, higher currents are required to generate the necessary heat for the PbTe/Ni reaction at the interface, which could damage the PbTe [25]. No reaction was observed at 30 MPa, whereas Fig. 1(b) and (c) illustrates the interphase obtained at 10 and 20 MPa, respectively, using 250 A and 10 s of welding time. Pressures as high as 30 MPa substantially decrease the contact resistance, indicating that electrical currents higher than 250 A would be required to initiate the PbTe/Ni reaction. On the other hand, the contact area between Ni and PbTe at pressures as low as 10 MPa are shown to be insufficient to generate a continuous diffusion barrier layer (Fig. 1(b)), and geometrical instability has caused cracks between the layers. The intermediate pressure of 20 MPa was found to be the optimum value (Fig. 1(c)) to join Ni and PbTe without defects. Nonetheless, further optimisation of the bonding time was needed to generate a smooth diffusion layer at the contact.

The welding time needs to be sufficient to generate enough heat for the reaction, but excess time leads to over-heating and expulsion of material. In order to investigate the heat supplied by SPS, or equally the Joule heating released by the assembly, temperatures were recorded during each of the bonding processes. The thermocouple used for temperature data collection is situated inside the graphite punch and roughly 3 mm below the Ni/PbTe contact area. The difficulties associated with accurate reading of the reaction temperature are due to radiation losses from the sample and the quick release of heat at the Ni/PbTe contact area, which makes the temperature to oscillate (Figure S2 of the Supporting Information). These

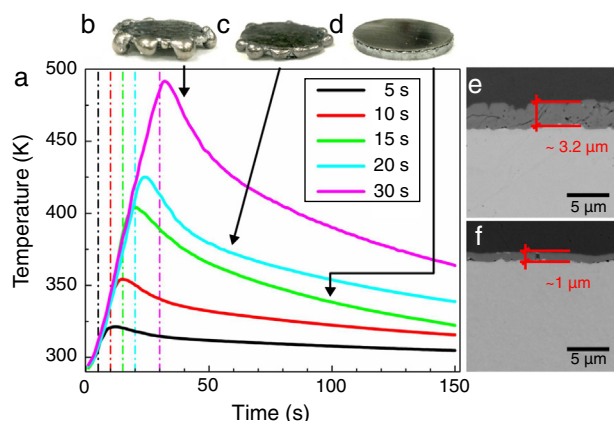


Fig. 2 – (a) Temperature over time for increasing welding times of 5, 10, 15, 20, and 30 s. Vertical dashed lines indicate the welding time for each process. It is observed that there is a delay in the maximum peak of the temperature reading by the thermocouple compared to their respective welding times. Photographs of pellets after bonding at 30, 20, and 15 s are presented in (b), (c), and (d), respectively. Micrographs showing the interphase formed after 15 and 20 s are presented in (e) and (f), respectively.

oscillations are caused by the equipment's proportional, integral, derivative (PID) controller and the intermittent release of heat from the Ni/PbTe contact area [20]. Similarly, the current method entails shorter bonding times, thus indicating lower temperatures than with the previous temperature-controlled SPS bonding method where it was optimised at 648 K (see Figure S2(a) of the Supporting Information). Fig. 2 shows the measured temperatures during and after bonding as a function of time for different bonding times, with photographs of relevant pellets, as well as the fabricated interphase layers after bonding times of 15 and 20 s in Fig. 2(e) and (f), respectively. The measured thermocouple temperature (solid lines) increases with welding time, with its maximum peak recorded by the thermocouple a few seconds after the respective bonding time was completed (with dashed lines indicating the bonding time). This delay occurred due to heat conduction through the sample and punch before reaching the tip of the thermocouple [20] (see details of the assembly in Figure S1 of Supporting Information). Samples bonded for 5 and 10 s presented no reaction, so that quick separation of layers occurred after removing the assembly from the SPS. This might be associated with insufficient Joule heating to induce reaction at the contact. Fig. 1(c), however, shows that 10 s of bonding time were sufficient in that case for a partial reaction along the contact. This discrepancy in the bonding results after 10 s of welding time, with the interphase formed shown in Fig. 1(c), is likely to be caused by either slight differences in surface qualities between the samples or the sensitivity of the SPS electronic functions. The employed SPS 10-4 apparatus is intended to supply high values of amperage with a maximum at 4000 A, and operating at 6% (250 A) of total power is not recommended due to non-linear output from the transformers and rectifiers in the equipment's electronics. It is worth noting that slightly rougher contact surfaces, as on the sample shown

in Fig. 1(b) can affect the bonding by providing extra contact resistance, so more Joule heating is provided for the reaction. The thickness and surface quality of workpieces determine the reproducibility of results. In this study, the initial thicknesses of the Ni plate and bulk PbTe were carefully obtained at 0.27 and 1.5 mm, respectively, with both surfaces mechanically polished down to 1 μm and ultrasonically cleaned to remove possible oxide residue. Nevertheless, it is a common practice in welding processes to tune the initial welding conditions to deal with small variations in the surface quality or oxidation of layers.

Successful bonding was achieved after the remarkable welding time of 15 s, compared to 5 min [20] or an hour [19] in our previous studies. Reports of Ni/PbTe bonding using HP [28] or plasma activated sintering (PAS) [29] indicate that much higher temperatures and times were required for sintering. The former method was performed at 873 K for 120 min to generate sporadic intermetallic particles along the contact between elements [28], while the latter technique involved bonding at 1050 K for 540 s, with the sample demonstrating good electrical contact, with no sharp change in the voltage potential at the Ni/PbTe transition area [30]. No clear micrograph of the interface was provided, however.

Fig. 2(d) shows that 15 s of welding time is necessary to observe molten material spatter from the Ni/PbTe contact, which is indicative of optimal conditions. In addition, Fig. 2(e) presents an SEM image of the cross-section of the sample in Fig. 2(d), where a smooth and continuous interlayer has been formed. This interphase is 3.2 μm thick, so that it can efficiently act as a diffusion barrier layer separating Ni from PbTe. Fig. 2(b) and (c) presents samples obtained at 20, and 30 s. These holding times resulted in extensive expulsion of molten material from the interface, as indicated by the solidified bubbles on the samples' periphery, affecting their total geometries (separation of layers at 30 s) and reduced interlayer thickness (20 s welding time). This is in agreement with the RSW process, where melt expulsion of the weld nugget can result in porosity and even separation of bonded metal sheets during solidification [31]. Similarly, it is also due to melt expulsion that a decrease in the interphase thickness is observed from 3 μm in Fig. 2(e) for 15 s to 1 μm in Fig. 2(f) for 20 s. Nevertheless, this bonding procedure requires that Pb, a by-product of the reaction, is expelled so to form a continuous and flawless diffusion barrier [19]. Simultaneously, the holding time must be short enough to avoid melting of the bulk PbTe.

Fig. 3 presents the homogenous interphase generated at the interface in Ni/PbTe cross-sections, which were successfully bonded using the parameters 250 A, 20 MPa, and 15 s. Table 1 shows the chemical compositions of areas designated in Fig. 3 as Ni, β_2 Ni_{3±x}Te₂, and PbTe, respectively, from top

Table 1 – Chemical compositions (atomic percentages) of the areas presented in Fig. 3.

Areas	Ni (at.%)	Te (at.%)	Pb (at.%)
Ni	100	–	–
Ni ₃ Te ₂	61.6	37.5	0.9
PbTe	–	49.5	50.5

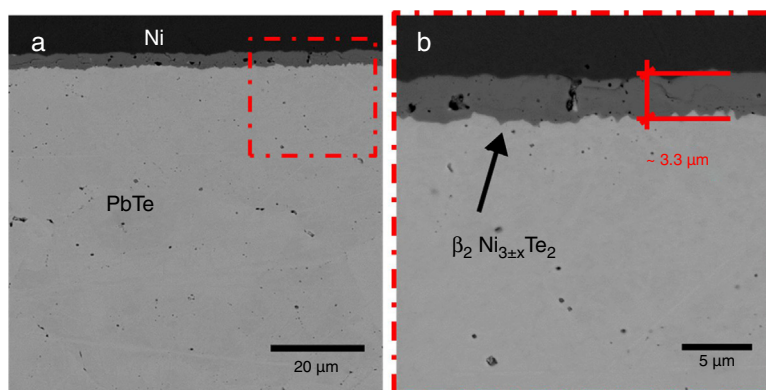


Fig. 3 – (a) Backscattered micrograph of samples welded at 250 A, 20 MPa, and 15 s. (b) Magnification of the interphase in (a) showing smooth generation of a diffusion barrier layer across the sample with the interfacial composition of β_2 Ni₃Te₂.

to bottom. The interphase layer is identified as monoclinic Ni₃Te₂, which has crystallographic equivalence to the higher tetragonal crystal symmetry [20]. In this particular bonding procedure, based on controlling the electrical current, we are capable of forming an extremely thin effective diffusion barrier layer, which adds a small contribution to the total electrical contact resistance of the thermoelectric generator, thus improving the total performance. This reduction in average thickness of the interlayer to 3.3 μm while maintaining effective separation of layers is a significant improvement from previous studies that showed interphase thickness of roughly 27 μm [19] and 7 μm [20] (seen in Figure S3 of the Supporting Information). Additionally, chemical and mechanical stability of generated interphase were previously studied by ageing bonded sample of Ni, β_2 Ni_{3±x}Te₂, and n-type PbTe at 823 K for 360 h [19]. The study concluded good integrity of interphase layer, while PbTe showed signs of sublimation. Furthermore, the current SPS method performs exceptionally well in terms of the formation of a fine and effective interphase when compared to similar Ni/PbTe joins made via HP [28], where a non-continuous diffusion barrier layer is formed, limiting the device operating temperature due to the ongoing reaction between the layers.

Fig. 4 shows the linear behaviour of the V–I curve obtained from bonded Ni to n-type PbTe, indicating an ohmic contact. The total resistance of sample (0.8 mΩ) is obtained from the slope of the line in Fig. 4. The resistance for PbTe bulk corresponds to 0.53 mΩ, and that of Ni plate is 3.2×10^{-3} mΩ. Therefore, the resistance of interphase, Ni₃Te₂, and its contact with Ni and PbTe is equal to 273 μΩ.

4. Conclusions

We have introduced a current-controlled spark plasma sintering method to successfully bond Ni to PbTe in a few seconds, forming a thin 3 μm diffusion barrier layer. The substantial reduction in bonding time achieved by this new approach has improved the quality of the joined counterparts, with no cracks or porosity observed on the PbTe material. This current-controlled SPS technique, which resembles common resistance spot welding, utilises Joule heating at the contact

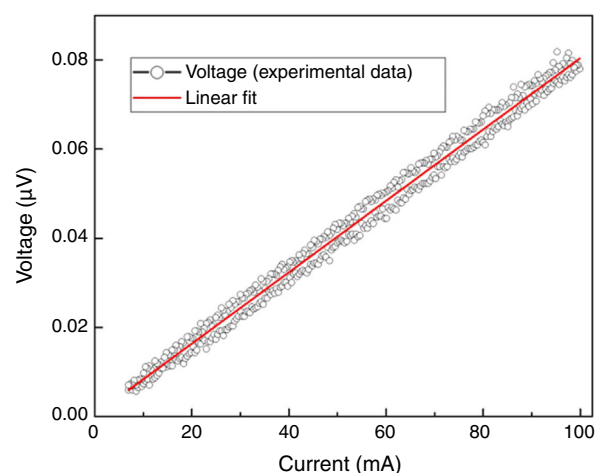


Fig. 4 – Measured voltage (solid circles) versus applied electrical current, showing a linear fit (solid red line) to the experimental data.

area of the workpieces to effectively generate the required interphase for high temperature thermoelectric devices. The obtained thin interphase is solely composed of β_2 Ni₃Te₂ phase.

Conflicts of interest

The authors declare no competing financial interests.

Acknowledgments

This work was supported by an Australian Research Council (ARC) Linkage Project (LP120200289), an ARC Discovery Early Career Award (DE130100310), and the AutoCRC (Project Agreement 1-203). The authors would like to thank the Electron Microscopy Centre (EMC) at the University of Wollongong for access to microscopes and sample preparation equipment.

Appendix A. Supplementary data

Supplementary data associated with this article can be found, in the online version, at [doi:10.1016/j.jmrt.2018.01.008](https://doi.org/10.1016/j.jmrt.2018.01.008).

REFERENCES

- [1] Ellabban O, Abu-Rub H, Blaabjerg F. Renewable energy resources: current status, future prospects and their enabling technology. *Renew Sustain Energy Rev* 2014;39:748–64.
- [2] Quadrelli R, Peterson S. The energy–climate challenge: recent trends in CO₂ emissions from fuel combustion. *Energy Policy* 2007;35(11):5938–52.
- [3] Bell LE. Cooling, heating, generating power, and recovering waste heat with thermoelectric systems. *Science* 2008;321(5895):1457–61.
- [4] Yeo IA, Yee JJ. A proposal for a site location planning model of environmentally friendly urban energy supply plants using an environment and energy geographical information system (E-GIS) database (DB) and an artificial neural network (ANN). *Appl Energy* 2014;119:99–117.
- [5] Andrić I, Jamali-Zghal N, Santarelli M, Lacarrière B, Le Corre O. Environmental performance assessment of retrofitting existing coal fired power plants to co-firing with biomass: carbon footprint and energy approach. *J Clean Prod* 2015;103:13–27.
- [6] Hosenuzzaman M, Rahim NA, Selvaraj J, Hasanuzzaman M, Malek ABMA, Nahar A. Global prospects, progress, policies, and environmental impact of solar photovoltaic power generation. *Renew Sustain Energy Rev* 2015;41:284–97.
- [7] Yodovard P, Khedari J, Hirunlabh J. The potential of waste heat thermoelectric power generation from diesel cycle and gas turbine cogeneration plants. *Energy Sources* 2001;23(3):213–24.
- [8] Rowe DM. Thermoelectrics, an environmentally-friendly source of electrical power. *Renew Energy* 1999;16(1–4):1251–6.
- [9] Snyder GJ. Small thermoelectric generators. *Electrochem Soc Interface* 2008;17(3):54.
- [10] Snyder GJ, Toberer ES. Complex thermoelectric materials. *Nat Mater* 2008;7(2):105–14.
- [11] Dughaish ZH. Lead telluride as a thermoelectric material for thermoelectric power generation. *Physica B Condens Matter* 2002;322(1–2):205–23.
- [12] Liu W, Jie Q, Kim HS, Ren Z. Current progress and future challenges in thermoelectric power generation: from materials to devices. *Acta Mater* 2015;87:357–76.
- [13] Lilyana K, Roumen K. Ohmic contacts for high power and high temperature microelectronics. In: Takahata K, editor. *Micro Electronic and Mechanical Systems*. Rijeka: InTech; 2009.
- [14] Rowe DM. *CRC handbook of thermoelectrics: macro to nano*. Boca Raton: CRC Taylor & Francis; 2006.
- [15] Bjørk R. The universal influence of contact resistance on the efficiency of a thermoelectric generator. *J Electron Mater* 2015;44(8):2869–76.
- [16] Kraemer D, Sui J, McEnaney K, Zhao H, Jie Q, Ren ZF, et al. High thermoelectric conversion efficiency of MgAgSb-based material with hot-pressed contacts. *Energy Environ Sci* 2015;8(4):1299–308.
- [17] Ngan PH, Van Nong N, Hung LT, Balke B, Han L, Hedegaard EMJ, et al. On the challenges of reducing contact resistances in thermoelectric generators based on half-Heusler alloys. *J Electron Mater* 2016;45(1):594–601.
- [18] Guillon O, Gonzalez-Julian J, Dargatz B, Kessel T, Schierning G, Räthel J, et al. Field-assisted sintering technology/spark plasma sintering: mechanisms, materials, and technology developments. *Adv Eng Mater* 2014;16(7):830–49.
- [19] Reales Ferreres X, Aminorroaya Yamini S, Nancarrow M, Zhang C. One-step bonding of Ni electrode to n-type PbTe – a step towards fabrication of thermoelectric generators. *Mater Des* 2016;107:90–7.
- [20] Reales Ferreres X, Gazder AA, Manettas A, Aminorroaya Yamini S. Solid-state bonding of bulk PbTe to Ni electrode for thermoelectric modules. *ACS Applied Energy Materials* 2018;1(2):348–54.
- [21] Podražaj P, Polajnar I, Diaci J, Kariž Z. Overview of resistance spot welding control. *Sci Technol Weld Join* 2008;13(3): 215–24.
- [22] Zhang H, Senkara J. *Resistance welding: fundamentals and applications*. Boca Raton, Florida: CRC Press; 2011.
- [23] Wan X, Wang Y, Zhang P. Modelling the effect of welding current on resistance spot welding of DP600 steel. *J Mater Process Technol* 2014;214(11):2723–9.
- [24] Muhammad N, Manurung YHP, Hafidzi M, Abas SK, Tham G, Haruman E. Optimization and modeling of spot welding parameters with simultaneous multiple response consideration using multi-objective Taguchi method and RSM. *J Mech Sci Technol* 2012;26(8):2365–70.
- [25] Jihui Y, Thierry C. Thermoelectric materials for space and automotive power generation. *MRS Bull* 2006;31(03):224–9.
- [26] Zhou K, Cai L. Study on effect of electrode force on resistance spot welding process. *J Appl Phys* 2014;116(8):084902.
- [27] Chang BH, Zhou Y. Numerical study on the effect of electrode force in small-scale resistance spot welding. *J Mater Process Technol* 2003;139(1–3):635–41.
- [28] Xia H, Drymiotis F, Chen CL, Wu A, Snyder GJ. Bonding and interfacial reaction between Ni foil and n-type PbTe thermoelectric materials for thermoelectric module applications. *J Mater Sci* 2014;49(4):1716–23.
- [29] Orihashi M, Noda Y, Chen L, Kang YS, Moro A, Hirai T. Electric properties of Ni/n-PbTe and Ni/p-Pb_{0.5}Sn_{0.5}Te joined by plasma activated sintering. In: *Materials science forum*; 1999.
- [30] Orihashi M, Noda Y, Chen L, Kang Y, Moro A, Hirai T. Ni/n-PbTe and Ni/p-Pb_{0.5}Sn_{0.5}Te joining by plasma activated sintering. In: *Proceedings of the 17th international conference on thermoelectrics (ICT'98)*. Nagoya, Japan: IEEE; 1998.
- [31] Pouranvari M, Asgari HR, Mosavizadch SM, Marashi PH, Goodarzi M. Effect of weld nugget size on overload failure mode of resistance spot welds. *Sci Technol Weld Join* 2007;12(3):217–25.